Sensors & Actuators: B. Chemical 432 (2025) 137488

Contents lists available at ScienceDirect

Sensors and Actuators: B. Chemical

journal homepage: www.elsevier.com/locate/snb

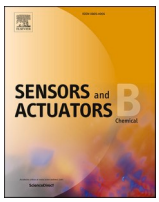

Detection of NH_3 impurities in H_2 environment exploiting quartz-enhanced photoacoustic spectroscopy with an optimized spectrophone

Chaofan Feng [a,b,c,1], Ruyue Cui [a,b,1], Giansergio Menduni [c], Andrea Zifarelli [c], Pietro Patimisco [a,c,d], Angelo Sampaolo [a,c,d], Vincenzo Spagnolo [a,c,d,*], Lei Dong [a,b,c,*], Hongpeng Wu [a,b,c,*]

[a] State Key Laboratory of Quantum Optics Technologies and Devices, Institute of Laser Spectroscopy, Shanxi University, Taiyuan 030006, China
[b] Collaborative Innovation Center of Extreme Optics, Shanxi University, Taiyuan 030006, China
[c] PolySense Lab—Dipartimento Interateneo di Fisica, University and Politecnico of Bari, Bari, Italy
[d] PolySense Innovations Srl, Bari, Italy

ARTICLE INFO

Keywords:
Hydrogen impurities
Ammonia
Gas sensors
QEPAS
Custom spectrophone

ABSTRACT

We report on a quartz-enhanced photoacoustic spectroscopy (QEPAS) sensor for ammonia impurities detection in hydrogen. A quantum cascade laser with a central emission wavelength of 9.062 μm was used to excite the NH_3 absorption line at 1103.44 cm^{-1}, with a linestrength of $1.51 \cdot 10^{-19}$ cm/molecule. Compared to detecting contaminants in ambient air, the distinct properties of hydrogen required the design of a dedicated QEPAS spectrophone optimized for operation in hydrogen-based mixtures. The custom-made spectrophone was composed by a QTF excited at the first overtone mode at 44 kHz, acoustically coupled with an easy-to-align, dual-tube amplification system. The custom-made spectrophone was implemented in a QEPAS sensor, achieving a minimum detection limit of 95 ppb with a lock-in integration time of 0.1 s. Furthermore, the Allan-Werle deviation analysis returned a detection limit as low as 1.5 ppb when for an integration time of 30 s.

1. Introduction

Hydrogen is currently one of the most studied energy sources for its sustainable properties and for its capability to efficiently replace traditional sources in energy production industry [1]. In particular, H_2 employed in fuel cells (FCs) does not produce greenhouse gases after its combustion, but in the process of preparing hydrogen, a variety of impurity gases could be produced [2]. Indeed, to ensure the performance of FCs, the hydrogen fuel quality standard set by ISO 14687:2019 specifies maximum allowable levels for 14 impurity gas molecules, including carbon monoxide, carbon dioxide, formaldehyde [3,4]. For example, the ammonia produced during hydrogen preparation and the NH_3 traces formed by the reaction of internal hydrogen and nitrogen during FCs operation could even poison the FCs [5]. Francisco A. Uribe et al.[6] found that when hydrogen containing 13 ppm ammonia impurities is filled into the fuel cells for 1 h, FCs performance gradually decreases. However, they can be fully recovered after 12 h, refilling FCs with pure H_2. Conversely, when the NH_3 impurity concentration reaches 30 ppm and the exposure time exceeded 15 h, the performances could not be restored to the original state within a few days, even refilling FCs with pure hydrogen. Therefore, the detection of traces of ammonia in hydrogen matrix is of great significance.

In recent years, ammonia impurities in H_2 have been detected mainly with Fourier transform infrared spectrometers, semiconductor devices or gas chromatographs [7–9]. However, these sensors are bulky and not suitable for exposure at high H_2 concentration, limiting the feasibility of in-situ detection and the operation in corrosive, reactive and dusty gas streams [10,11]. Recently, several laser-based optical techniques have been employed to measure NH_3 in real world applications, thus overcoming the abovementioned limits and at the same time achieving high sensitivity. In Ref. [12], a direct absorption spectroscopy apparatus was employed for in-situ and simultaneous detection of ammonia for selective catalytic reduction exhaust monitoring. A commercial analyser based on the cavity ring-down spectroscopy allowed the monitoring of

* Corresponding authors at: State Key Laboratory of Quantum Optics Technologies and Devices, Institute of Laser Spectroscopy, Shanxi University, Taiyuan 030006, China.
E-mail addresses: vincenzoluigi.spagnolo@poliba.it (V. Spagnolo), donglei@sxu.edu.cn (L. Dong), wuhp@sxu.edu.cn (H. Wu).
[1] These authors have contributed equally to this work.

https://doi.org/10.1016/j.snb.2025.137488
Received 27 November 2024; Received in revised form 28 January 2025; Accepted 19 February 2025
Available online 20 February 2025

NH_3 emissions in metropolitan areas, as described in Ref. [13]. Finally, the results shown in Ref. [14] are promising for measuring ammonia levels with tunable diode laser absorption spectroscopy in flue gas treatments processes. Although the reported examples have not been directly tested in hydrogen-based matrix, the architecture of the sensing system can be easily adapted for this task. Furthermore, also optical sensor based on Quartz enhanced photoacoustic spectroscopy (QEPAS) can overcome these issues [15–18]. This technique can be used to detect traces of NH_3 in H_2 matrix by exploiting the photoacoustic effect: when intensity-modulated light is tuned to a wavelength that matches a radiative transition of NH_3, sound waves can be generated within the H_2 matrix. This occurs due to the non-radiative relaxation of excited NH_3 molecules, which transfer energy to collisional H_2 neighbors. In QEPAS, these sound waves are detected by a spectrophone, composed by a quartz tuning fork (QTF) and a pair of resonator tubes, fully immersed in the gas mixture [19]. QEPAS sensors have already demonstrated high performance in trace gas detection within N_2 and ambient environments. With their fast response and small footprint, they have become effective tools for real-time and in situ trace gas detection in different industrial applications [20–25]. The potentiality of the extension of the QEPAS technique for trace gas detection in H_2 environments stems directly from its fundamental detection principle. The signal is generated by deformations of the QTF prongs due to the impact of sound waves. In other words, the QTF works as a passive detector, namely without need for external polarization, avoiding the risk of generating uncontrolled electrical discharges within the gas sample. This, combined with quartz's resistance to corrosion in high-concentration hydrogen environments, allows QEPAS to be safely used for detecting contaminants in H_2 environments. Also, when a QTF vibrates in hydrogen, it can achieve a significantly higher quality factor compared to standard air or nitrogen environments. This increase in quality factor is largely due to the lower density of hydrogen, which results in reduced damping forces on the vibrating QTF. Consequently, this enhanced vibrational efficiency in H_2 could lead to improved sensitivity and performance.

In this work, we report on a QEPAS sensor for detection of NH_3 in H_2. The NH_3 absorption feature at 1103.44 cm^{-1} with a linestrength of $1.51{\cdot}10^{-19}$ cm/molecule was excited by a quantum cascade laser (QCL) [26]. A comprehensive investigation revealed the inefficiency of the commercially available spectrophone, which consists of a T-shaped QTF with a fundamental resonance frequency of 12.4 kHz, coupled with two resonator tubes measuring 1.24 cm in length. This configuration represents a state-of-the-art spectrophone widely used for trace gas detection in nitrogen-based environments [27,28]. We demonstrated that the different sound speed in H_2 with respect to N_2 necessitates a re-design of the spectrophone, with the need to operate at a higher resonance frequency by exciting the first overtone mode of a custom-made QTF. This enables the use of optimized tubes with a practical length of approximately ~ 1 cm, allowing for detection performance of NH_3 in H_2 to match that expected in an N_2 environment.

2. Experimental setup

The QEPAS sensor for detection of NH_3 in H_2 is reported in Fig. 1. A distributed-feedback QCL (Thorlabs, Model QD9062HH) with a central emission wavelength of 9.062 μm was used to excite NH_3 molecules. The NH_3 absorption line at 1103.44 cm^{-1} was targeted by setting the QCL temperature to 41°C and injecting a current of 392.4 mA by using a Thorlabs combo-controller (Model ITC4002QCL). Under these operating conditions, an emission power of 39.8 mW was measured at the exit of the QCL. A ZnSe lens with a focal length of 50 mm was used to focus the collimated laser beam into the Acoustic Detection Module (ADM), a stainless-steel chamber with two windows that houses the QEPAS spectrophone. The lens directs the laser beam through resonator tubes, focusing it between the prongs of the QTF without touching them. A power meter was employed to assist with the optical alignment. The function generator (Tektronix, Model AFG 31052) was used to supply

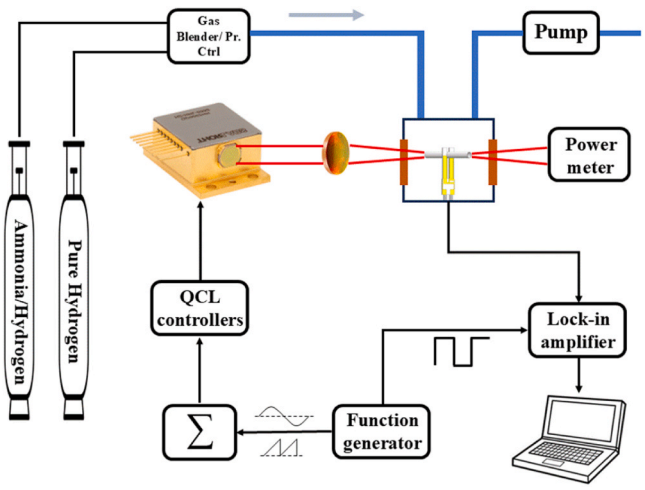

Fig. 1. Schematic of the QEPAS sensor for the detection of ammonia traces in hydrogen.

sine and triangle waves, combined with an adder, that drives the QCL controller and modulate the injected current. In detail, the triangle wave allows the full scan of the NH_3 absorption profile, while the sinewave enables the 2*f* wavelength modulation spectroscopy (2*f*-WMS) detection scheme. This method requires setting the sinewave frequency to half of the resonance frequency f_r of the QTF and demodulating the spectrophone signal at f_r using a lock-in amplifier (Zurich Instruments, Model MFLI). The integration time of the lock-in amplifier (τ) was set to 0.1 s and the signal acquisition time to 0.3 s. Finally, the flow conditions within the ADM were stabilized using a gas handling system composed of gas cylinders, a gas blender-pressure controller combo-unit (MCQ-INSTRUMENTS GM VACUUM 1.3) and a pump. For the QEPAS sensor calibration, a mixture of 13 ppm of NH_3:H_2 was diluted with a pure hydrogen cylinder. The gas blender was used to generate mixtures with different ammonia concentrations in hydrogen, as well as to stabilize the pressure and flow of the mixture within the ADM. All measurements were carried out at a flow rate of 50 sccm. This value was selected to ensure both minimal turbulence in the detection module [29] and reduced rise/decay time in sensor operation because of ammonia adsorption/desorption effects [30]. Using the experimental setup shown in Fig. 1, a rise time (10–90 %) of ~20 min was observed, while a decay time (90–10 %) of ~10 min was observed.

2.1. NH_3 traces detected in H_2-based mixtures using the state-of-the-art spectrophone

The state-of-the-art spectrophone (Thorlabs, ADM01) was first employed in the QEPAS sensor depicted in Fig. 1. It consists of a T-shaped QTF with a fundamental resonance frequency of 12.4 kHz coupled with a dual-tube amplification system. Each tube has a length of 12.4 mm with an inner radius a = 0.8 mm, and it is positioned 150 μm far from the QTF surface and Fig. 2 shows the QEPAS spectral scan of the NH_3 absorption profile acquired with the certified mixture of 13 ppm NH_3 in H_2 at a pressure of 100 Torr flowing through the ADM [31].

The shape of measured 2*f*-spectral scan is highly distorted and only faintly resembles the expected second-derivative of a Lorentzian function [32]. The observed spectral distortions cannot be attributed to spectral overlap with other absorption features, as the selected NH_3 line is well isolated from potential interferents, such as condensed water vapor in the gas line. Simulations of the NH_3 absorption feature at 100 Torr further confirm the presence of a distinct, isolated peak [26]. Additionally, these distortions are not a result of fringes or artifacts typically associated with poor optical alignment or suboptimal laser beam quality, as spectral scans obtained with pure H_2 flow through the

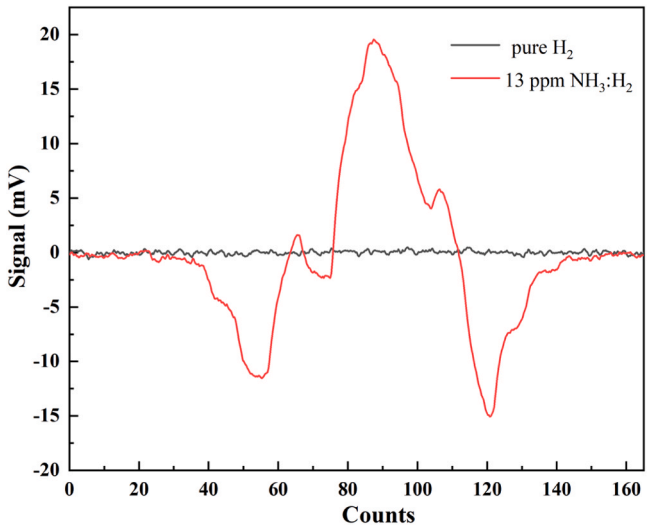

Fig. 2. QEPAS spectral scan of a mixture containing pure hydrogen (black curve) and 13 ppm NH_3:H_2 at 100 Torr (red curve), acquired with the state-of-the-art spectrophone (ADM01, Thorlabs).

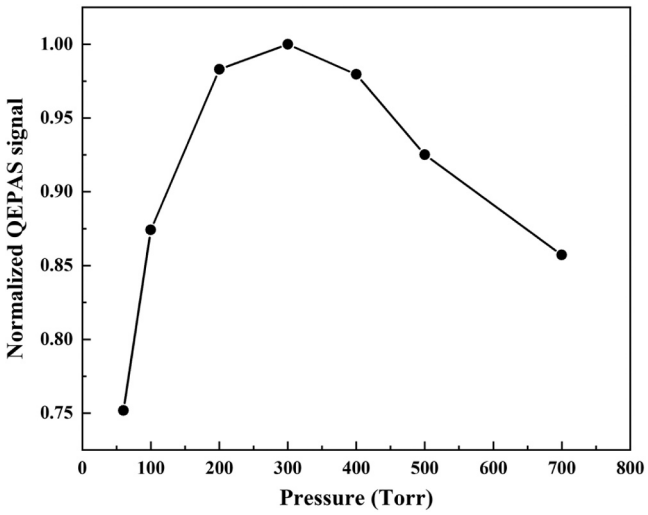

Fig. 3. Normalized QEPAS signal peaks of 13 ppm NH_3:H_2 in the 50–700 Torr pressure range for the 12.4 kHz T-shaped QTF.

ADM were background-free. Consequently, the deformations in the spectral scans are attributed to acoustic coupling effects between the tube resonator system and the QTF. The state-of-the-art spectrophone is assembled in an on-beam configuration, with the QTF positioned between the tubes. The acoustic amplification within tubes is most effective when the tube length is properly chosen, allowing multiple reflected waves from the ends of the resonator constructively interfere and form a standing wave acoustic pattern. Considering the open-end correction, the length of each tube (l) is correlated with the sound wavelength by the following [33]:

$$l = \frac{v_s}{2f_r} - \frac{16a}{3\pi} \quad (1)$$

where v_s is the speed of sound in the environment. The tube length of the state-of-the-art spectrophone is optimized for operation in an ambient environment, resulting in $l = 12.4$ mm for a speed of sound $v_s = 343$ m/s in air with $f_r = 12.4$ kHz. Moving to hydrogen environment, the speed of sound increases to 1330 m/s at room temperature and atmospheric pressure [34]. Using Eq. (1), the optimal tube length results 54 mm for $f_r = 12.4$ kHz, nearly 4 times the length of the tube in the state-of-the-art spectrophone. For this reason, we removed the resonator tubes from the spectrophone and only bare T-shaped QTF was employed as sound wave detector in the ADM.

The QEPAS spectral scan of the NH_3 absorption feature was acquired at different pressures with the certified concentration of 13 ppm NH_3:H_2 injected into the ADM at 50 sccm. The normalized peak value of each spectral scan was plotted as a function of the pressure in Fig. 3.

The strongest QEPAS signal was achieved at an operating pressure of 300 Torr, where the QTF exhibited a resonance frequency of 12.457 kHz and a quality factor of 51300. The QEPAS sensor calibration was performed by introducing various ammonia concentrations into the gas line. These concentrations were achieved by diluting the certified 13 ppm NH_3:H_2 gas cylinder with pure hydrogen. The resulting QEPAS spectral scans are displayed in Fig. 4a, and the extracted peak values at different ammonia concentrations are plotted in Fig. 4b.

The comparison between the spectral scan shapes in Fig. 4a and that obtained using a state-of-the-art spectrophone (Fig. 2) confirms the initial hypothesis: the observed spectral distortion is primarily due to non-optical acoustic coupling between the tubes and the QTF, mainly resulting from the incorrect tube length. This is further evident in the peak values of the spectral scans. With a certified concentration of 13 ppm of NH_3 in H_2, the bare T-shaped QTF yields a QEPAS peak signal of 2.7 mV (Fig. 4a). This is notably lower than the peak signal of 20 mV achieved with the state-of-the-art spectrophone (see Fig. 2) with the same mixture in the ADM. Consequently, the resonator tubes enhance the QEPAS signal by a factor of approximately 7.4, which is anyway significantly below the typical amplification achieved in air or N_2 of around 60 [31]. However, for optimal performance, a QEPAS sensor should operate under conditions that enable a clear reconstruction of the absorption feature, free from distortions that can introduce fringe patterns, as in Fig. 2. This is because such deformations can alter the peak value, which is the key parameter for determining trace gas concentrations in a matrix, as well as the ultimate detection limit of the sensor. Thus, we evaluated the ultimate performance of the QEPAS sensor employing the bare T-shaped QTF in the ADM. Considering the slope of the linear fit 0.23 mV/ppm (with R-square value of 0.97) in Fig. 4b, and a 1σ noise level of 0.16 mV (measured as the standard deviation of the QEPAS signal when pure hydrogen flows in the ADM) a minimum detection limit (MDL) of ~700 ppb was calculated. The long-term stability of the QEPAS sensor was assessed using the Allan-Werle deviation analysis. This measurement was performed flowing pure hydrogen in the ADM at a pressure of 300 Torr and setting the laser emission wavelength at the ammonia absorption peak. The obtained MDL in ppm-unit as a function of the lock-in integration time is shown in Fig. 5.

Aside from a slight increase at short integration times, the MDL follows the expected $1/\sqrt{\tau}$-like trend for $\tau > 1$ s, up to 100 s where the sensor reaches an MDL of ~20 ppb [35].

2.2. *NH_3 traces detected in H_2-based mixtures using the overtone mode of an I-shaped QTF*

The design of a spectrophone optimized for use in hydrogen environment can be derived by analyzing Eq. (1). For frequencies in the kHz range, the contribution of the second term can be disregarded, allowing us to omit the tube diameter from this discussion. With this assumption, the main constraint is given by the tube length, which must be limited to ~ 1.5 centimeters to facilitate the optical alignment. This means that the resonance frequency must be adjusted when the speed of sound, or the surrounding environment, varies in the ADM. Starting from the tube length $l = 1.24$ cm of the state-of-the-art spectrophone, a QTF with a resonance frequency of ~48 kHz must be used, 3.9 times higher than of the T-shaped QTF, exactly as the ratio between the speed of sound in hydrogen and that in the air. To demonstrate our assumptions, among all the custom QTFs we previously employed in QEPAS sensors [36–38], we identified the QTF with rectangular prongs, labelled as QTF#2 in

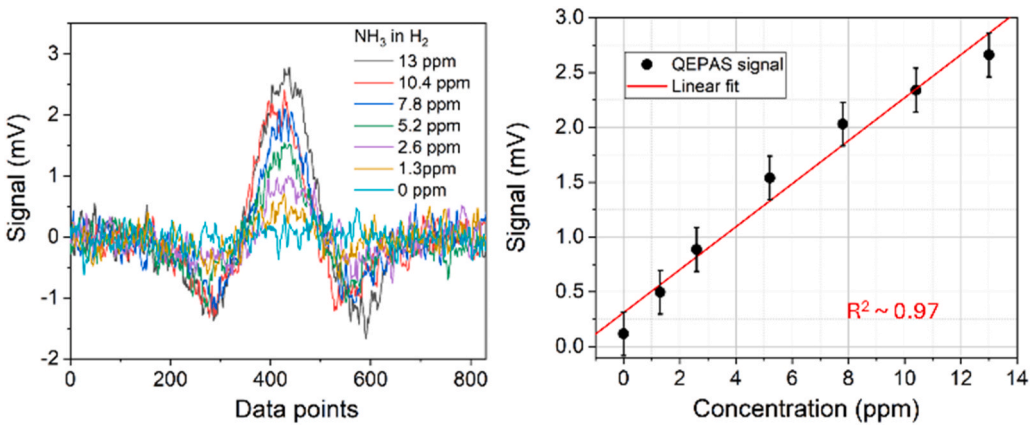

Fig. 4. (a) 2*f*-QEPAS signals collected under different concentrations of NH_3 diluted in H_2. (b) Calibration curve of the QEPAS sensor. The black dots represent the experimental data, the red line represents the linear fitting curve.

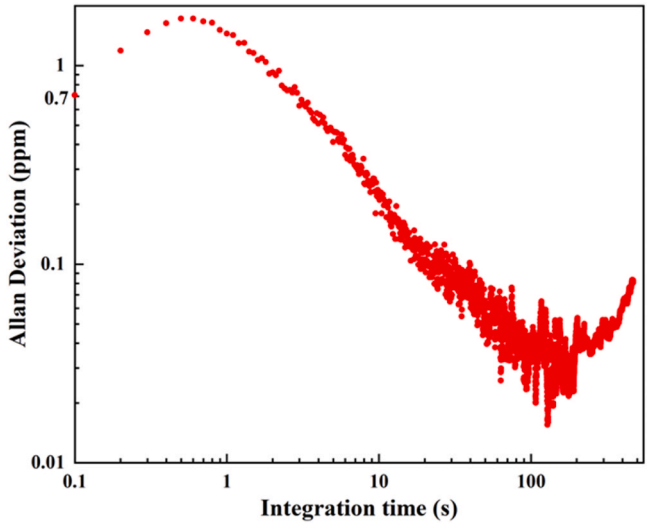

Fig. 5. Allan-Werle deviation analysis for the ammonia detection with the T-shaped QTF.

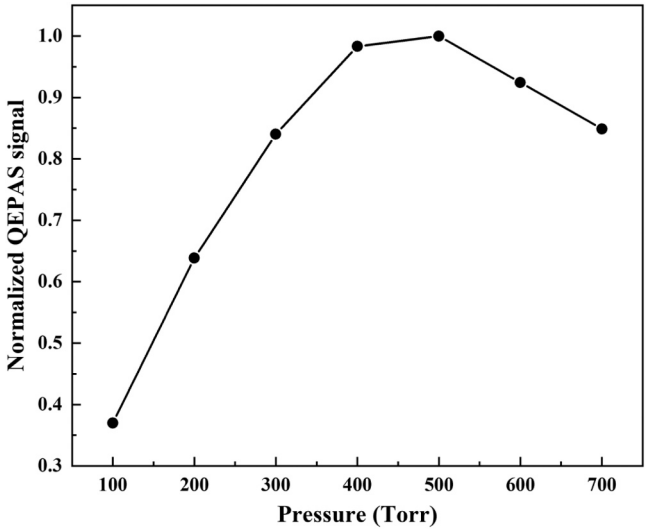

Fig. 6. Normalized QEPAS signal peaks of 13 ppm NH_3:H_2 in the 100–700 Torr pressure range measured exciting the first overtone mode of the custom-made spectrophone.

Ref. [36]. This resonator has prongs length, thickness and spacing of 10 mm, 0.9 mm and 0.8 mm, respectively, with a quartz crystal thickness of 0.25 mm. The tuning fork exhibits a resonance frequency of the fundamental mode at 7.6 kHz and the first overtone mode resonance frequency of ~ 44 kHz [34].

Using Eq. (1), the optimal tube length is $l_{44\ kHz} \sim 15.0$ mm when the first overtone mode is excited. Thus, QTF#2 was coupled with the resonator tubes employed in the Thorlabs-ADM01 (inner diameter of 1.6 mm and a length of 12.4 mm), in order to excite the upper antinode of the first overtone flexural mode of the QTF, mirroring the configuration of the state-of-the-art spectrophone. This assembly will be named hereafter as custom-made spectrophone. A ~15 % difference in tube length from the optimal size is not expected to significantly affect the overall performance of the QEPAS sensor, as already demonstrated in previous works [31,39].

The custom-made spectrophone was mounted in the ADM to be used in the experimental setup of Fig. 1 for detecting NH_3 trace in H_2. Using the same procedure described before, the trend of the QEPAS peak signal of the NH_3 absorption feature was analyzed at various pressures, as shown in Fig. 6.

The optimal pressure maximizing the QEPAS signal results 500 Torr, higher than the value found for the state-of-the-art spectrophone (300 Torr), with a resonance frequency and a quality factor of the spectrophone of 44.135 kHz and 43170, respectively. An increase of the optimal pressure is expected when shifting to higher frequencies. For optimal signal conditions, the excitation frequency should allow the excited NH_3 molecules to effectively transfer excess energy to surrounding H_2 molecules. As the excitation frequency increases, a faster energy relaxation rate is required, meaning that a greater density of surrounding molecules—achieved through higher pressure—is necessary to maintain efficient overall energy transfer[40].

The calibration of the sensor was carried out at 500 Torr: the QEPAS spectral scans for different ammonia concentrations in hydrogen and the extracted peak values as a function of ammonia concentration are reported in Fig. 7a and 7b, respectively.

As expected, the 2*f*-scans do not exhibit any distortion, confirming that the acoustic coupling between QTF#2 and resonator tubes is optimal. Moreover, the linear fit of the datapoints in Fig. 7b returns a R-square value of 0.996, higher than that obtained with bare T-shaped QTF (0.97). Considering the slope 1.8 mV/ppm of the linear fit and a 1σ noise level of 0.17 mV, an MDL of ~95 ppb was achieved with 0.1 s lock-in integration time. This result can be qualitatively compared with the best achievement obtained with QEPAS for NH_3 detection in N_2 by targeting the same absorption line, reporting an MDL of 5.8 ppb [41]. The net comparison indicates a reduction in MDL by a factor of

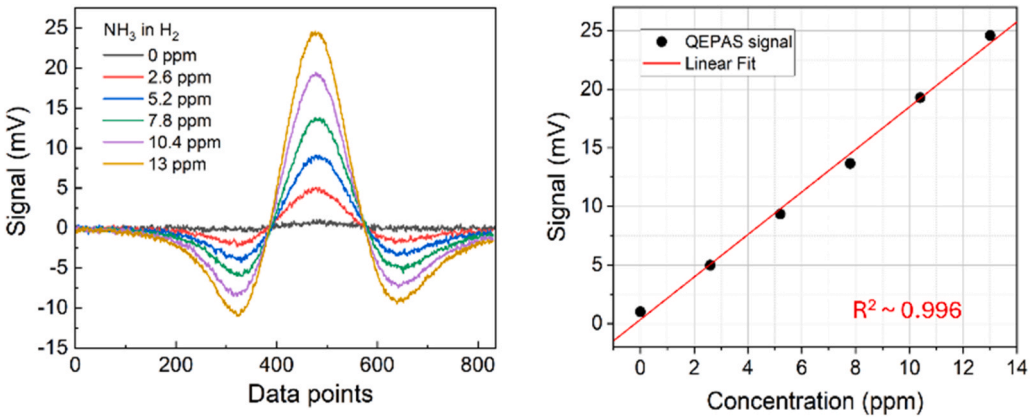

Fig. 7. (a) 2*f*-QEPAS signals collected under different concentrations of NH_3 diluted in H_2. (b) Calibration curve of the QEPAS sensor. The black dots represent the experimental data, the red line represents the linear fitting curve. The error bars fall within the experimental data point symbols.

approximately 16. Emphasizing the performance differences between the two QTFs helps to clarify much of this discrepancy. As detailed in Ref. 33, a thorough comparison of QEPAS performance across different QTFs reveals that the signal-to-noise ratio of a bare T-shaped QTF is approximately eight times higher than that of QTF#2 when operating in its fundamental mode. However, to fully account for the observed discrepancy, additional factors must be considered. When shifting from the fundamental mode to a high-frequency overtone mode (>40 kHz), the performance of a QTF in a QEPAS sensor generally declines. Additionally, the signal enhancement provided by resonator tubes varies between different QTF designs.

Finally, the long-term stability of the sensor was assessed with the Allan-Werle deviation analysis shown in Fig. 8.

The MDL has $1/\sqrt{\tau}$-like trend up to integration time of 30 s, with a corresponding detection limit of 1.5 ppb. The different behavior between Fig. 5 and Fig. 8 at integration times from 0.1 s up to 1 s is mainly due to the different response of the electronic components at the two resonance frequencies.

3. Conclusions

In this work, we developed a QEPAS sensor optimized for detecting trace ammonia (NH_3) in hydrogen (H_2)-based mixtures. Traditional spectrophones, designed for air-based environments, proved inadequate in hydrogen due to the significantly higher speed of sound, which disrupts acoustic coupling with the QTF. Using an analytical model to examine acoustic interactions in hydrogen, we designed a spectrophone comprising a custom QTF operating at its first overtone mode (44 kHz) and coupling it with resonator tubes of 12.4 mm length, facilitating reliable optical alignment even with suboptimal laser beam quality. The optimized spectrophone achieved a minimum detection limit (MDL) of 95 ppb for NH_3 in hydrogen at 500 Torr and with a 0.1 s integration time. Stability analysis via Allan-Werle deviation confirmed that the MDL could be further reduced to 1.5 ppb with a 30 s integration, highlighting the sensor's stability and sensitivity. This advancement not only underscores the potential of QEPAS for hydrogen environments but also supports future custom QTF designs for sensitive gas trace detection in hydrogen and a deeper understanding of resonator acoustic coupling in H_2-based matrices. Additionally, this optimized approach could be extended to detect other contaminants specified in the ISO 14687:2019 standard for hydrogen fuel purity [4]. Future research on ammonia detection will prioritize mitigating adsorption/desorption effects on the sensor walls. This will include examining the impact of varying flow rates on the QEPAS signal and developing experimental approaches to increase and stabilize the detection system temperature, ensuring accuracy, and long-term reliability in diverse operating conditions.

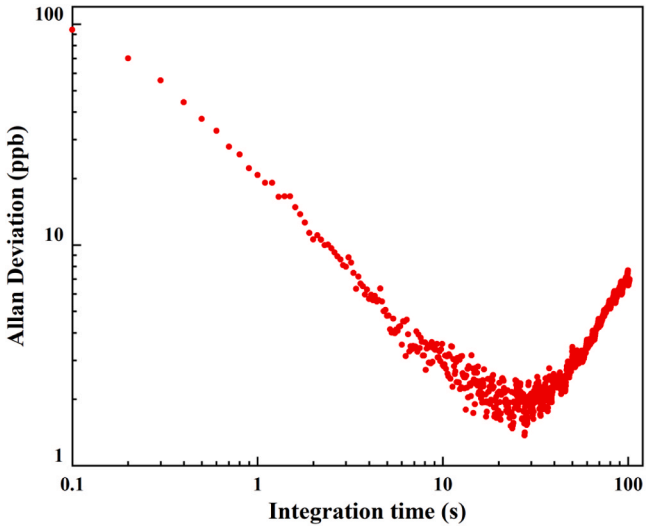

Fig. 8. Allan-Werle deviation analysis for the ammonia detection with the custom-made spectrophone.

CRediT authorship contribution statement

Menduni Giansergio: Writing – original draft, Methodology, Conceptualization. **Cui Ruyue:** Methodology, Data curation. **Feng Chaofan:** Writing – original draft, Investigation, Data curation. **Patimisco Pietro:** Writing – review & editing, Methodology, Funding acquisition. **Wu Hongpeng:** Writing – review & editing, Supervision, Methodology, Conceptualization. **Dong Lei:** Writing – review & editing, Supervision, Funding acquisition, Conceptualization. **Spagnolo Vincenzo:** Writing – review & editing, Supervision, Funding acquisition, Conceptualization. **Sampaolo Angelo:** Writing – review & editing, Methodology, Investigation, Conceptualization. **Zifarelli Andrea:** Data curation.

Declaration of Competing Interest

The authors declare that they have no known competing financial interests or personal relationships that could have appeared to influence the work reported in this paper.

Acknowledgments

The project is supported by National Natural Science Foundation of China (NSFC) [grant numbers 62475137, 62122045, 62075119,

62235010, 62175137]; The Shanxi Science Fund for Distinguished Young Scholars (20210302121003); Shanxi Provincial Special Fund for Scientific and Technological Cooperation and Exchange (202304041101019); Fundamental Research Program of Shanxi Province, China (Grant No. 202403021212183). The authors from Dipartimento Interateneo di Fisica di Bari acknowledge financial support from PNRR MUR project PE0000023-NQSTI, project MUR – Dipartimenti di Eccellenza 2023–2027 – Quantum Sensing and Modelling for One-Health (QuaSiModO) and THORLABS GmbH within the PolySenSe joint research laboratory. Andrea Zifarelli and Pietro Patimisco acknowledge financial support from the project "HIGAS - Development of a Hydrogen Impurity Gas Analyzer based on quartz-enhanced photoacoustic Spectroscopy" (D33C22001330002) within the framework of PNRR MUR project PE0000021-NEST - Network 4 Energy Sustainable Transition.

Data Availability

Data will be made available on request.

References

[1] A. Bartle, Hydropower potential and development activities, Energy Policy 30 (2002) 1231–1239, https://doi.org/10.1016/S0301-4215(02)00084-8.
[2] B. Shadidi, G. Najafi, T. Yusaf, A review of hydrogen as a fuel in internal combustion engines, Energies 14 (2021) 6209, https://doi.org/10.3390/EN14196209.
[3] A. Murugan, A.S. Brown, Review of purity analysis methods for performing quality assurance of fuel cell hydrogen, Int. J. Hydrog. Energy 40 (2015) 4219–4233, https://doi.org/10.1016/J.IJHYDENE.2015.01.041.
[4] T. Stöhr, V. Reiter, S. Scheikl, N. Klopčič, S. Brandstätter, A. Trattner, Hydrogen quality in used natural gas pipelines: an experimental investigation of contaminants according to ISO 14687:2019 standard, Int. J. Hydrog. Energy 67 (2024) 1136–1147, https://doi.org/10.1016/J.IJHYDENE.2023.09.305.
[5] R. Halseid, P.J.S. Vie, R. Tunold, Effect of ammonia on the performance of polymer electrolyte membrane fuel cells, J. Power Sources 154 (2006) 343–350, https://doi.org/10.1016/J.JPOWSOUR.2005.10.011.
[6] F.A. Uribe, S. Gottesfeld, T.A. Zawodzinski, Effect of ammonia as potential fuel impurity on proton exchange membrane fuel cell performance, J. Electrochem Soc. 149 (2002) A293, https://doi.org/10.1149/1.1447221/XML.
[7] W. Deng, F. Deng, T. Zhang, J. Lin, L. Zhao, G. Li, Y. Pan, J. Yang, Continuous measurement of reactive ammonia in hydrogen fuel by online dilution module coupled with Fourier transform infrared spectrometer, Chin. Chem. Lett. (2024) 110085, https://doi.org/10.1016/J.CCLET.2024.110085.
[8] N.X. Thai, N. Van Duy, N. Van Toan, C.M. Hung, N. Van Hieu, N.D. Hoa, Effective monitoring and classification of hydrogen and ammonia gases with a bilayer Pt/SnO2 thin film sensor, Int. J. Hydrog. Energy 45 (2020) 2418–2428, https://doi.org/10.1016/J.IJHYDENE.2019.11.072.
[9] C. Beurey, B. Gozlan, M. Carré, T. Bacquart, A. Morris, N. Moore, K. Arrhenius, H. Meuzelaar, S. Persijn, A. Rojo, A. Murugan, Review and Survey of Methods for Analysis of Impurities in Hydrogen for Fuel Cell Vehicles According to ISO 14687: 2019, Front Energy Res. 8 (2021) 615149, https://doi.org/10.3389/FENRG.2020.615149/BIBTEX.
[10] L. Dong, W. Ma, F.K. Tittel, H. Wu, X. Yin, L. Zhang, W. Yin, L. Xiao, S. Jia, Highly sensitive photoacoustic multicomponent gas sensor for SF_6 decomposition online monitoring, Opt. Express 27 (4) (2019) A224–A234, https://doi.org/10.1364/OE.27.00A224.
[11] S. Zampolli, I. Elmi, J. Stürmann, S. Nicoletti, L. Dori, G.C. Cardinali, Selectivity enhancement of metal oxide gas sensors using a micromachined gas chromatographic column, Sens. Actuators B Chem. 105 (2005) 400–406, https://doi.org/10.1016/J.SNB.2004.06.036.
[12] Y. Ji, K. Duan, Z. Lu, W. Ren, Mid-infrared absorption spectroscopic sensor for simultaneous and in-situ measurements of ammonia, water and temperature, Sens. Actuators B Chem. 371 (2022) 132574, https://doi.org/10.1016/j.snb.2022.132574.
[13] J. Heo, P. Kim, J. Park, J.Y. Lee, Source identification of ultrafine particulate matter and ammonia emissions in the metropolitan area, 240074–0, Environ. Eng. Res. 30 (2024), https://doi.org/10.4491/eer.2024.074.
[14] H. Wang, X. Shi, K. Li, Y. Yu, Z. Wang, J. Kang, Simulation and experimental research on trace detection of ammonia escape based on TDLAS, Infrared Phys. Technol. 127 (2022) 104458, https://doi.org/10.1016/j.infrared.2022.104458.
[15] B. Li, G. Menduni, M. Giglio, P. Patimisco, A. Sampaolo, A. Zifarelli, H. Wu, T. Wei, V. Spagnolo, L. Dong, Quartz-enhanced photoacoustic spectroscopy (QEPAS) and Beat Frequency-QEPAS techniques for air pollutants detection: a comparison in terms of sensitivity and acquisition time, Photoacoustics 31 (2023) 100479, https://doi.org/10.1016/j.pacs.2023.100479.
[16] B. Sun, A. Zifarelli, H. Wu, S. Dello Russo, S. Li, P. Patimisco, L. Dong, V. Spagnolo, Mid-infrared quartz-enhanced photoacoustic sensor for ppb-Level CO detection in a SF 6 gas matrix exploiting a t-grooved quartz tuning fork, Anal. Chem. 92 (2020) 13922–13929, https://doi.org/10.1021/acs.analchem.0c02772.
[17] A. Zifarelli, R. De Palo, S. Venck, F. Joulain, S. Cozic, R. Weih, A. Sampaolo, P. Patimisco, V. Spagnolo, All-fiber-coupled mid-infrared quartz-enhanced photoacoustic sensors, Opt. Laser Technol. 176 (2024) 110926, https://doi.org/10.1016/j.optlastec.2024.110926.
[18] M. Yang, Z. Wang, H. Sun, M. Hu, P.T. Yeung, Q. Nie, S. Liu, N. Akikusa, W. Ren, Highly sensitive QEPAS sensor for sub-ppb N2O detection using a compact butterfly-packaged quantum cascade laser, Appl. Phys. B 130 (2024) 1–8, https://doi.org/10.1007/S00340-023-08140-6/FIGURES/8.
[19] H. Lin, Y. Liu, L. Lin, W. Zhu, X. Zhou, Y. Zhong, M. Giglio, A. Sampaolo, P. Patimisco, F.K. Tittel, J. Yu, V. Spagnolo, H. Zheng, Application of standard and custom quartz tuning forks for quartz-enhanced photoacoustic spectroscopy gas sensing, Appl. Spectrosc. Rev. 58 (2023) 562–584, https://doi.org/10.1080/05704928.2022.2070917.
[20] A. Sampaolo, G. Menduni, P. Patimisco, M. Giglio, V.M.N. Passaro, L. Dong, H. Wu, F.K. Tittel, V. Spagnolo, Quartz-enhanced photoacoustic spectroscopy for hydrocarbon trace gas detection and petroleum exploration, Fuel 277 (2020), https://doi.org/10.1016/j.fuel.2020.118118.
[21] Quartz-Enhanced Photoacoustic Sensor for Methane, (n.d.). ⟨https://www.thorlabs.com/newgrouppage9.cfm?objectgroup_id= 16188⟩ (accessed November 27, 2024).
[22] K. Kinjalk, F. Paciolla, B. Sun, A. Zifarelli, G. Menduni, M. Giglio, H. Wu, L. Dong, D. Ayache, D. Pinto, A. Vicet, A. Baranov, P. Patimisco, A. Sampaolo, V. Spagnolo, Highly selective and sensitive detection of volatile organic compounds using long wavelength InAs-based quantum cascade lasers through quartz-enhanced photoacoustic spectroscopy, Appl. Phys. Rev. 11 (2024), https://doi.org/10.1063/5.0189501/3298456.
[23] C. Feng, B. Li, Y. Jing, J. Wang, P. Patimisco, V. Spagnolo, A. Sampaolo, L. Dong, H. Wu, Enrichment-enhanced photoacoustic spectroscopy based on vertical graphene, Sens. Actuators B Chem. 417 (2024) 136204, https://doi.org/10.1016/J.SNB.2024.136204.
[24] H. Wu, L. Dong, H. Zheng, X. Liu, X. Yin, W. Ma, L. Zhang, W. Yin, S. Jia, F.K. Tittel, Enhanced near-infrared QEPAS sensor for sub-ppm level H2S detection by means of a fiber amplified 1582 nm DFB laser, Sens. Actuators B Chem. 221 (2015) 666–672, https://doi.org/10.1016/J.SNB.2015.06.049.
[25] H. Wu, L. Dong, H. Zheng, Y. Yu, W. Ma, L. Zhang, W. Yin, L. Xiao, S. Jia, F. K. Tittel, Beat frequency quartz-enhanced photoacoustic spectroscopy for fast and calibration-free continuous trace-gas monitoring, 2017 8:1, Nat. Commun. 8 (2017) 1–8, https://doi.org/10.1038/ncomms15331.
[26] I.E. Gordon, L.S. Rothman, R.J. Hargreaves, R. Hashemi, E.V. Karlovets, F. M. Skinner, E.K. Conway, C. Hill, R.V. Kochanov, Y. Tan, P. Wcisło, A.A. Finenko, K. Nelson, P.F. Bernath, M. Birk, V. Boudon, A. Campargue, K.V. Chance, A. Coustenis, B.J. Drouin, J.M. Flaud, R.R. Gamache, J.T. Hodges, D. Jacquemart, E.J. Mlawer, A.V. Nikitin, V.I. Perevalov, M. Rotger, J. Tennyson, G.C. Toon, H. Tran, V.G. Tyuterev, E.M. Adkins, A. Baker, A. Barbe, E. Canè, A.G. Császár, A. Dudaryonok, O. Egorov, A.J. Fleisher, H. Fleurbaey, A. Foltynowicz, T. Furtenbacher, J.J. Harrison, J.M. Hartmann, V.M. Horneman, X. Huang, T. Karman, J. Karns, S. Kassi, I. Kleiner, V. Kofman, F. Kwabia-Tchana, N. N. Lavrentieva, T.J. Lee, D.A. Long, A.A. Lukashevskaya, O.M. Lyulin, V. Y. Makhnev, W. Matt, S.T. Massie, M. Melosso, S.N. Mikhailenko, D. Mondelain, H. S.P. Müller, O.V. Naumenko, A. Perrin, O.L. Polyansky, E. Raddaoui, P.L. Raston, Z. D. Reed, M. Rey, C. Richard, R. Tóbiás, I. Sadiek, D.W. Schwenke, E. Starikova, K. Sung, F. Tamassia, S.A. Tashkun, J. Vander Auwera, I.A. Vasilenko, A.A. Vigasin, G.L. Villanueva, B. Vispoel, G. Wagner, A. Yachmenev, S.N. Yurchenko, The HITRAN2020 molecular spectroscopic database, J. Quant. Spectrosc. Radiat. Transf. 277 (2022), https://doi.org/10.1016/J.JQSRT.2021.107949.
[27] THORLABS ADM01 ⟨https://www.thorlabs.com/newgrouppage9.cfm?objectgroup_id= 2940⟩, (n.d.). ⟨https://www.thorlabs.com/newgrouppage9.cfm?objectgroup_id= 2940⟩.
[28] M. Giglio, A. Elefante, P. Patimisco, A. Sampaolo, F. Sgobba, H. Rossmadl, V. Mackowiak, H. Wu, F.K. Tittel, L. Dong, V. Spagnolo, Quartz-enhanced photoacoustic sensor for ethylene detection implementing optimized custom tuning fork-based spectrophone, Opt. Express 27 (2019) 4271–4280, https://doi.org/10.1364/oe.27.004271.
[29] A. Zifarelli, G. Negro, L.A. Mongelli, A. Sampaolo, E. Ranieri, L. Dong, H. Wu, P. Patimisco, G. Gonnella, V. Spagnolo, Effect of gas turbulence in quartz-enhanced photoacoustic spectroscopy: a comprehensive flow field analysis, Photoacoustics 38 (2024) 100625, https://doi.org/10.1016/j.pacs.2024.100625.
[30] G. Menduni, A. Zifarelli, E. Kniazeva, S. Dello Russo, A.C. Ranieri, E. Ranieri, P. Patimisco, A. Sampaolo, M. Giglio, F. Manassero, E. Dinuccio, G. Provolo, H. Wu, D. Lei, V. Spagnolo, Measurement of methane, nitrous oxide and ammonia in atmosphere with a compact quartz-enhanced photoacoustic sensor, Sens Actuators B Chem. 375 (2023) 132953, https://doi.org/10.1016/j.snb.2022.132953.
[31] F.K. Tittel, A. Sampaolo, V. Mackowiak, A. Cable, P. Patimisco, V. Spagnolo, S. dello Russo, H. Rossmadl, M. Giglio, Tuning forks with optimized geometries for quartz-enhanced photoacoustic spectroscopy, Vol. 27, Issue 2, Pp. 1401-1415, Opt. Express 27 (2019) 1401–1415, https://doi.org/10.1364/OE.27.001401.
[32] P. Patimisco, A. Sampaolo, Y. Bidaux, A. Bismuto, M. Scott, J. Jiang, A. Muller, J. Faist, F.K. Tittel, V. Spagnolo, Purely wavelength- and amplitude-modulated quartz-enhanced photoacoustic spectroscopy, Opt. Express 24 (2016) 25943, https://doi.org/10.1364/oe.24.025943.
[33] S. Dello Russo, M. Giglio, A. Sampaolo, P. Patimisco, G. Menduni, H. Wu, L. Dong, V.M.N. Passaro, V. Spagnolo, Acoustic coupling between resonator tubes in quartz-enhanced photoacoustic spectrophones employing a large prong spacing tuning fork, Sensors (Switzerland) 19 (2019), https://doi.org/10.3390/s19194109.

[34] L. Dong, J. Wright, B. Peters, B.A. Ferguson, F.K. Tittel, S. McWhorter, Compact QEPAS sensor for trace methane and ammonia detection in impure hydrogen, Appl. Phys. B 107 (2012) 459–467, https://doi.org/10.1007/S00340-012-4908-X/FIGURES/12.
[35] M. Giglio, P. Patimisco, A. Sampaolo, G. Scamarcio, F.K. Tittel, V. Spagnolo, Allan Deviation plot as a tool for quartz-enhanced photoacoustic sensors noise analysis, IEEE Trans. Ultrason Ferroelectr. Freq. Control 63 (2016) 555–560, https://doi.org/10.1109/TUFFC.2015.2495013.
[36] F.K. Tittel, A. Sampaolo, P. Patimisco, L. Dong, A. Geras, T. Starecki, V. Spagnolo, Analysis of overtone flexural modes operation in quartz-enhanced photoacoustic spectroscopy, (2016). https://doi.org/10.1364/OE.24.00A682.
[37] P. Patimisco, A. Sampaolo, L. Dong, M. Giglio, G. Scamarcio, F.K. Tittel, V. Spagnolo, Analysis of the electro-elastic properties of custom quartz tuning forks for optoacoustic gas sensing, Sens. Actuators B Chem. 227 (2016) 539–546, https://doi.org/10.1016/j.snb.2015.12.096.
[38] P. Patimisco, A. Sampaolo, V. Mackowiak, H. Rossmadl, A. Cable, F.K. Tittel, V. Spagnolo, Loss mechanisms determining the quality factors in quartz tuning forks vibrating at the fundamental and first overtone modes, IEEE Trans. Ultrason Ferroelectr. Freq. Control 65 (2018) 1951–1957, https://doi.org/10.1109/TUFFC.2018.2853404.
[39] P. Patimisco, A. Sampaolo, H. Zheng, L. Dong, F.K. Tittel, V. Spagnolo, Quartz–enhanced photoacoustic spectrophones exploiting custom tuning forks: a review, Adv. Phys. X 2 (2017) 169–187, https://doi.org/10.1080/23746149.2016.1271285.
[40] M. Olivieri, M. Giglio, S. Dello Russo, G. Menduni, A. Zifarelli, P. Patimisco, A. Sampaolo, H. Wu, L. Dong, V. Spagnolo, Assessment of vibrational-translational relaxation dynamics of methane isotopologues in a wet-nitrogen matrix through QEPAS, Photoacoustics 31 (2023) 100518, https://doi.org/10.1016/j.pacs.2023.100518.
[41] R. De Palo, A. Elefante, G. Biagi, F. Paciolla, R. Weih, V. Villada, A. Zifarelli, M. Giglio, A. Sampaolo, V. Spagnolo, P. Patimisco, Quartz-enhanced photoacoustic sensors for detection of eight air pollutants, Adv. Photonics Res. 4 (2023), https://doi.org/10.1002/adpr.202200353.

Chaofan Feng is now pursuing a Ph.D. degree in atomic and molecular physics in the Institute of Laser Spectroscopy of Shanxi University, China. His research interests include gas sensors, photoacoustic spectroscopy, and laser spectroscopy techniques.

Ruyue Cui received her dual Ph.D. degrees in physics from Shanxi University, China, and Université du Littoral Côte d'Opale, France, in 2023. Currently, she is a lecturer at the Institute of Laser Spectroscopy at Shanxi University. Her research interests encompass optical sensors and laser spectroscopy techniques.

Lei Dong received his Ph.D. degree in optics from Shanxi University, China, in 2007. From June, 2008 to December, 2011, he worked as a post-doctoral fellow in the Electrical and Computer Engineering Department and Rice Quantum Institute, Rice University, Houston, USA. Currently he is a professor in the Institute of Laser Spectroscopy of Shanxi University. His research activities research activities are focused on research and development in laser spectroscopy, in particular photoacoustic spectroscopy applied to sensitive, selective and real-time trace gas detection, and laser applications in environmental monitoring, chemical analysis, industrial process control, and medical diagnostics. He has published more than 100 peer reviewed papers with > 2200 positive citations.

Hongpeng Wu received his Ph.D. degree in atomic and molecular physics from Shanxi niversity, China, in 2017. From 2015–2016, he studied as a joint Ph.D. student in the electrical and computer engineering department and rice quantum institute, Rice University, Houston, USA. Currently he is a professor in the Institute of Laser Spectroscopy of Shanxi University. His research interests include optical sensors and laser spectroscopy techniques.

Giansergio Menduni received the M. S. degree (cum laude) in 2017 and the Ph.D. degree in 2021 in Electronic Engineering from the Polytechnic University of Bari. Since 2022, he is an Assistant Professor in Applied Physics at the Physics Department of Polytechnic University of Bari. His research activity is focused on the development of gas sensors based on Quartz-Enhanced Photoacoustic Spectroscopy (QEPAS) and Light-Induced Thermoelastic Spectroscopy (LITES) on the signal conditioning of Quartz Tuning Forks transducers.

Pietro Patimisco obtained the Master degree in Physics (cum laude) in 2009 and the PhD Degree in Physics in 2013 from the University of Bari. Since 2023, he is an associate professor at the Physics Department of University of Bari. He was a visiting scientist in the Laser Science Group at Rice University in 2013 and 2014. The main scientific skills of Pietro Patimisco are related to the development of spectroscopic techniques for studying the light-matter interaction in the infrared range. Prof. Pietro Patimisco is co-founder of "PolySenSe Innovations", a company devoted to the development of optical-based sensors.

Spagnolo Vincenzo received the degree (summa cum laude) and the PhD, both in physics, from University of Bari. He works as Full Professor of Applied Physics at the Technical University of Bari. In 2019, he become Vice-Rector of the Technical University of Bari, deputy to Technology Transfer. Since 2017, he is the director of the joint-research lab PolySense, created by THORLABS GmbH and Technical University of Bari, devoted to the development and implementation of novel gas sensing techniques and the realization of highly sensitive QEPAS trace-gas sensors.

Angelo Sampaolo obtained his Master degree in Physics in 2013 and the PhD Degree in Physics in 2017 from University of Bari. He was an associate researcher in the Laser Science Group at Rice University from 2014 to 2016 and associate researcher at Shanxi University since 2018. Since 2024, he is Associate Professor at Polytechnic of Bari. His research activity has focused on the development of innovative techniques in trace gas sensing, based on Quartz-Enhanced Photoacoustic Spectroscopy.

Andrea Zifarelli received the M.S. degree (cum laude) in Physics in 2018 from the University of Bari and his Ph.D. in Physics from the same institution in 2022. His research activities were mainly focused on the development of spectroscopic techniques based on laser absorption for the analysis of complex gas mixtures by employing quartz tuning forks as sensitive elements. This investigation was performed by using innovative laser sources as well as developing new algorithms for multivariate analysis approaches. Since 2024, he is Assistant Professor at University of Bari and his research activities are carried out at the PolySenSe Lab, joint-research laboratory between Technical University of Bari and THORLABS GmbH.